ACI STRUCTURAL JOURNAL TECHNICAL PAPER

Title no. 109-S50

# Constitutive Model for Fiber-Reinforced Polymer- and Tie-Confined Concrete

by Konstantinos G. Megalooikonomou, Giorgio Monti, and Silvia Santini

*The fiber-reinforced polymer (FRP)-confined concrete model proposal by* fib *was enhanced to take into account the confining effect of the already-existing steel reinforcement when retrofitting a reinforced concrete (RC) column with FRP jacketing. To this end, confining pressures contributed at each step of deformation by the case of existing transverse and longitudinal steel reinforcement were evaluated, considering the stress-strain law of the reinforcing steel. Moreover, the compatibility of strain in the lateral direction between the jacketing system and the encased concrete was enforced. Finally, the bilinear stress-strain response of FRP-confined concrete was terminated by jacket rupture, owing to hoop strains exceeding the strain capacity of the material or to interaction of the jacket with the buckled longitudinal bars. Correlation with three experimental studies was performed to validate the proposed iterative procedure.*

**Keywords:** buckling; circular section; confinement; fiber-reinforced polymer; model; steel ties; stress-strain behavior.

## INTRODUCTION

Confining wraps or jackets to rehabilitate and strengthen existing concrete columns has proven to be an efficient technique for the seismic retrofit of structures. However, most of the compressive strength models of confined concrete only consider the increased strength and ductility provided by fiber-reinforced polymers (FRPs), neglecting the contribution of the existing steel reinforcement inside the column's section. Even if the existing steel stirrups in a reinforced concrete (RC) column are not sufficient to confine the concrete core, they must contribute, along with the FRP jacket, to confining the section. Therefore, the FRP-confined concrete model proposal by *fib*[1] was enhanced to take into account the confining effect of the already-existing steel reinforcement when retrofitting an RC column with FRP jacketing. To this end, confining pressures contributed at each step of deformation by the case of existing transverse and longitudinal steel reinforcement were evaluated, considering the stress-strain law of the reinforcing steel. Finally, the compatibility of strain in the lateral direction between the jacketing system and the encased concrete was enforced.

## RESEARCH SIGNIFICANCE

Through the described approach, the differences in the lateral behavior of the concrete cover (confined with the jacket's pressure) and the concrete core (confined by both the steel's and FRP's pressure) were considered. This also allows the application of the model in cases of reinforcement repair and FRP retrofit, where two different concrete strengths should be considered: one for the new layer of concrete applied externally and the other for the old concrete in the concrete core, which may also be cracked due to former seismic loading.

## ANALYTICAL INVESTIGATION

### Modeling of concrete confined with steel and FRP

The behavior of confined circular sections under axial load is characterized by the radial lateral dilation, which causes radial confining forces or other axisymmetric passive confining pressure to increase with the amount of lateral expansion. Considering this scheme for the case of confinement by means of FRP jacketing (Fig. 1), to define the confining pressure acting on the section, it is necessary to define the jacket strain—or circumferential strain—parallel to the fibers' orientation. Relating the circumferential strain $\varepsilon_c$ to the strain in the radial direction $\varepsilon_r$, the following simple relationship is obtained, where $R$ is the radius of the circular section, $\Delta C$ is the change in the circumference of the circular section, and $C$ is the circumference of the circular section

$$\varepsilon_c = \frac{\Delta C}{C} = \frac{2\pi R(1+\varepsilon_r - 1)}{2\pi R} = \varepsilon_r \tag{1}$$

Owing to the axisymmetry of the problem, the outcome is that the circumferential strain and the strain in the radial direction are equal. This property has been extensively used to directly calculate the radial confining forces based on experimental data by strain gauges attached parallel to the fibers' orientation to obtain the circumferential strains. Along this line, it seems useful to try and extend the aforementioned simple calculation to the case where steel stirrups and external FRP jacketing are simultaneously present (Fig. 1). The steel ties divide the section into two parts: the first is the concrete core and the second is the concrete cover, where $R_{core}$ is the radius of the concrete core, $c$ is the concrete cover, $\varepsilon_{r.core}$ is the radial strain of the concrete core of the circular section, and $\varepsilon_{r.cover}$ is the radial strain of the concrete cover of the circular section.

$$\varepsilon_c = \frac{\Delta C}{C} = \frac{2\pi\left\{\left[R_{core}\left(1+\varepsilon_{r.core}\right)+c\left(1+\varepsilon_{r.cover}\right)\right]-\left(R_{core}+c\right)\right\}}{2\pi\left(R_{core}+c\right)} = \frac{R_{core}\left(1+\varepsilon_{r.core}\right)+c\left(1+\varepsilon_{r.cover}\right)}{\left(R_{core}+c\right)} - 1 \tag{2}$$

*ACI Structural Journal*, V. 109, No. 4, July-August 2012.
MS No. S-2010-338.R2 received October 2, 2011, and reviewed under Institute publication policies. Copyright © 2012, American Concrete Institute. All rights reserved, including the making of copies unless permission is obtained from the copyright proprietors. Pertinent discussion including author's closure, if any, will be published in the May-June 2013 *ACI Structural Journal* if the discussion is received by January 1, 2013.

*ACI member* **Konstantinos G. Megalooikonomou** *is a PhD Candidate at the University of Rome (Roma Tre), Rome, Italy. He received his diploma from Demokritus University of Thrace, Xanthi, Greece; and his MS from the ROSE School at the University of Pavia, Pavia, Italy. His research interests include seismic strengthening of concrete structures using fiber-reinforced polymer (FRP) composites and nonlinear structural analysis.*

**Giorgio Monti** *is a Full Professor at the Sapienza University of Rome, Rome, Italy, where he also received his diploma and PhD. He received his MS from the University of California at Berkeley, Berkeley, CA. His research interests include the modeling and analysis of reinforced concrete structures; strengthening techniques for structures with innovative materials, such as FRP; and reliability analysis of structures and infrastructures in seismic zones.*

**Silvia Santini** *is an Assistant Professor at the University of Rome, where she also received her diploma and PhD. Her research interests include strengthening strategies and techniques for reinforced concrete structures and infrastructures in seismic zones.*

As explicitly stated previously, the equation of radial strains and jacket strains for the case of both FRP- and steel-confined concrete in circular sections is no longer valid. The circumferential strain of the external jacket is based on the radial strains of both the concrete cover and concrete core, where in the latter, the presence of the steel ties plays an important role.

## Numerical model

The mechanical properties of concrete (strength, ductility, and energy dissipation) are substantially enhanced under a triaxial stress state. In practice, to develop a similar stress state, closed stirrups or spiral reinforcement are used so that, together with the longitudinal reinforcement, the lateral expansion of concrete is limited. This kind of (passive) confinement affects the behavior of the material favorably after the initiation of internal cracking, which gives rise to the initiation of expansion. For low strain values, the stress state in the transverse steel reinforcement is very small and the concrete is basically unconfined. In this range, steel and FRP jacketing behave similarly—that is, the inward pressure as a reaction to the expansion of concrete increases continuously. Therefore, speaking in terms of variable confining pressures corresponding to the axial strain level in the section and active triaxial models defining axial stress-strain curves for concrete subject to constant lateral pressure, it can be stated that the stress-strain curve describing the stress state of the section has to cross all active confinement curves up to the curve with lateral pressure equal to the one applied by the stirrups at yielding. Beyond yielding of stirrups, the lateral pressure still increases only due to the FRP jacketing, whereas the steel lateral pressure remains constant. The corresponding stress-strain curve of the section throughout this procedure converges to a confined-concrete axial stress-strain curve that is associated with a lateral pressure magnitude equal to the tensile strength of the FRP jacket plus the yielding strength of ties (excluding the strain-hardening behavior of steel because the ultimate strains of steel are usually much higher than those of FRP jackets). To model this behavior, an existing FRP-confined concrete model[2] has been enhanced to include the steel ties' contribution and thus model, in a more consistent way, circular columns with transverse reinforcement retrofitted with FRP jacketing. The previous model was based on an iterative procedure that needed to be modified, as shown in Fig. 2. In the procedure depicted in Fig. 2, after imposing an axial strain $\varepsilon_{con}$ on the section, a pressure coming from the FRP jacket $f_{l.cover}$ was assumed. Then, the Poisson's coefficient $\nu(\varepsilon_{con})$ until yielding of steel stirrups and the pressure coming from the steel ties $f_{l.steel}$ were calculated based on the

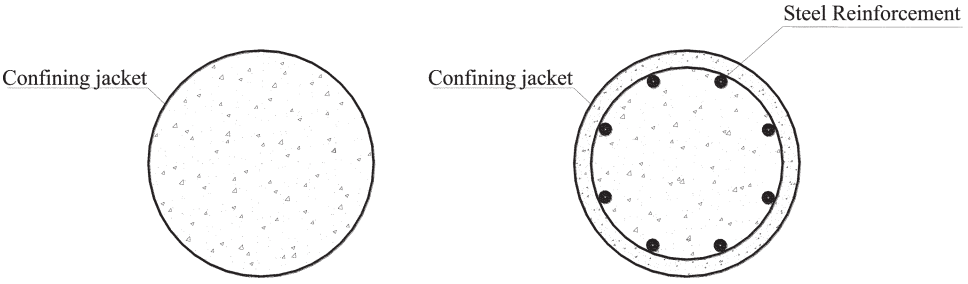


*Fig. 1—Circular section confined by steel stirrups and/or FRP jacket.*

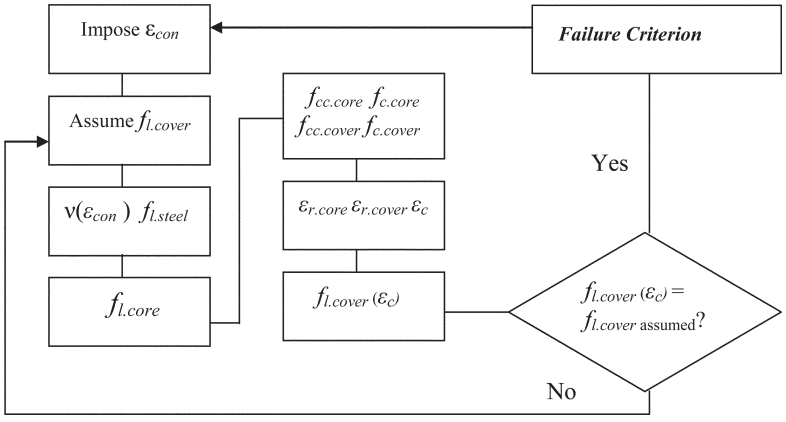


*Fig. 2—Iterative procedure.*

**Table 1—Equations embodied in iterative procedure**

| | |
|---|---|
| Braga et al.[3] | $f_{l.steel}(\varepsilon_{con}) = k_{sl}\dfrac{E_{con.core}E_s A_{sh}\nu(\varepsilon_{con})}{R_{core}E_{con.core}S + E_s A_{sh}[1-\nu(\varepsilon_{con})]\cdot[\nu(\varepsilon_{con})\cdot\varepsilon_{con}+1]}\cdot\varepsilon_{con}, \varepsilon_{sh} \le \varepsilon_{yh}$<br>$f_{l.steel}(\varepsilon_{con}) = k_{sl}0.5\rho_{sh}f_{yh}, \varepsilon_{shu} \ge \varepsilon_{sh} \ge \varepsilon_{yh}$<br>$\rho_{sh} = \dfrac{4A_{sh}}{D_{core}S},\ \varepsilon_{yh} = \dfrac{f_{yh}}{E_s},\ \varepsilon_{sh} = \varepsilon_{c.core} = \varepsilon_{r.core} = \nu(\varepsilon_{con})\cdot\varepsilon_{con}$<br>$\nu(\varepsilon_{con}) = \nu_o\left[1+0.2\left(\dfrac{\varepsilon_{con}}{\varepsilon_{co}}\right)-\left(\dfrac{\varepsilon_{con}}{\varepsilon_{co}}\right)^2+1.55\left(\dfrac{\varepsilon_{con}}{\varepsilon_{co}}\right)^3\right],\ \nu_o = 0.2,\ \varepsilon_{co} = 0.002$<br>$k_{sl} = \dfrac{45\xi_l{}^3}{45\xi_l{}^3+\eta\xi_{st}}, \xi_l = \dfrac{D_b}{S}, \eta = \dfrac{D_h}{D_b}, \xi_{st} = \dfrac{2D_h}{\pi R_{core}}$ |
| Spoelstra and Monti[2] | $f_c = \dfrac{f_{cc}\cdot x\cdot r}{r-1+x^r},\ x = \dfrac{\varepsilon_{con}}{\varepsilon_{cc}},\ \varepsilon_{cc} = \varepsilon_{co}\left[1+5\left(\dfrac{f_{cc}}{f_{co}}-1\right)\right],\ r = \dfrac{E_{con}}{E_{con}-E_{sec}},\ E_{sec} = \dfrac{f_{cc}}{\varepsilon_{cc}},\ \dfrac{f_{cc}(f_l)}{f_{co}} = 2.254\sqrt{1+7.94\dfrac{f_l}{f_{co}}}-2\dfrac{f_l}{f_{co}}-1.254,$<br>$\varepsilon_r(\varepsilon_{con}, f_l) = \dfrac{E_{con}\varepsilon_{con}-f_c(\varepsilon_{con}, f_l)}{2\beta f_c(\varepsilon_{con}, f_l)},\ \beta = \dfrac{5700}{\sqrt{\lvert f_{co}\rvert}}-500,\ E_{con} = 5700\cdot\sqrt{\lvert f_{co}\rvert}$ (MPa) |
| 14th *fib* Bulletin[1] | $k_j = \dfrac{\left(1-\dfrac{S_j}{2D}\right)^2}{1-\dfrac{A_b}{A_g}} \approx \left(1-\dfrac{S_j}{2D}\right)^2$ (coefficient for partial wrapping)<br>$f_{l.cover} = \dfrac{1}{2}k_j\rho_j E_j\varepsilon_c,\ \rho_j = \dfrac{4t_j}{D}$ |
| Iterative procedure | $f_{l.core} = f_{l.cover} + f_{l.steel},\ f_{c.av} = \dfrac{A_{core}}{A_{tot}}f_{c.core} + \dfrac{A_{cover}}{A_{tot}}f_{c.cover}$ |
| Bae et al.[7] | $\varepsilon_{sl} = \max\left[\left(\dfrac{0.035\cos\theta+\theta}{\cos\theta-0.035\theta}\right)\dfrac{u}{D_b}, \left(\dfrac{0.07\cos\theta+\theta}{\cos\theta-0.07\theta}\right)\left(\dfrac{u}{D_b}-0.035\right)\right],\ \theta = \dfrac{6.9}{(L_{buck}/D_b)^2}-0.05,\ \varepsilon_{sl} = \varepsilon_{con}$ |

BGL model.[3] Here, the longitudinal bars' contribution and the arching action between two adjacent stirrups along the column were also taken into account according to that model (refer to Table 1). The confining pressure in the concrete core $f_{l.core}$ is simply the summation of the lateral pressures contributed by the two confining systems (FRP and steel). The *fib* model's proposal[1] (Table 1) beyond this point is basically used to define the remainder of the parameters declared previously, applying that model for the two different regions already mentioned (herein, the different concrete properties, concrete strength and modulus of elasticity—that the two regions might have—can be taken into account). The focal point of the procedure is in the last step, where the confining pressure of the jacket is defined based on the circumferential strain of Eq. (2). Finally, at this point, cases where partial wrapping is applied have also been included[1] (Table 1).

## Failure criterion—FRP-confined circular RC sections

It has been well-established in recent studies that the rupture strains/strengths measured in tests on FRP-confined cylindrical specimens fall substantially below those from flat coupon tensile tests. Several reasons have been suggested for the observed lower rupture strains in place, including[4-6]:

- Misalignment or damage to jacket fibers during handling and layup;
- The radius of curvature in FRP jackets on cylinders as opposed to flat tensile coupons;
- Near failure, the concrete is internally cracked, resulting in nonhomogeneous deformations. Due to this nonhomogeneity of deformations and the high loads exerted on the cracked concrete, local stress concentrations may occur in the FRP reinforcement; and

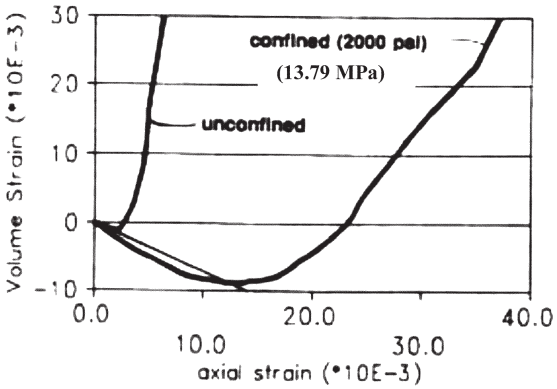


*Fig. 3—Volumetric strain versus axial compressive strain.*[10]

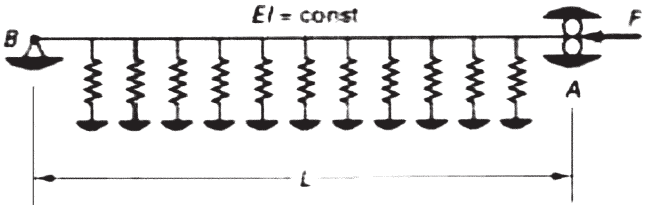


*Fig. 4—Pin-ended bar on elastic foundation.*

- The existence of a lap-splice zone, in which the measured strains are much lower than strains measured elsewhere.

Accounting for these effects, an ultimate tensile coupon FRP strain reduced by a *w* factor (ranging in the literature between 50 and 80%) is compared to the circumferential strain of concrete (Eq. (2)) and the ultimate compressive axial strain of concrete is considered to be attained when $\varepsilon_{j.rup.coup}$ is the rupture strain of tensile FRP coupons

$$\varepsilon_c \le w \cdot \varepsilon_{j.rup.coup} \tag{3}$$

## Failure criterion—FRP- and steel-confined circular RC sections

In old-type circular columns with inadequate transversal reinforcing details (where FRP jacketing is a commonly used remedy), the unsupported length of longitudinal bars (between two successive stirrups) is often much greater than $6D_b$ ($D_b$ is the diameter of the longitudinal bar). Therefore, the risk for buckling of longitudinal bars under compressive loads soon after yielding is higher. A dire implication is the reduced effectiveness of the FRP wraps due to interaction between the buckled longitudinal bars and the jacket, which may cause premature failure by rupture of the jacket.[8,9] This is an additional source of error contributing to the strength overestimation of FRP-confined concrete in addition to that generated by the difference between the nominal and in-place strain capacity of the wraps, as detailed previously. It is the objective of this paper to study the interaction between wraps and compression reinforcement in FRP-encased RC columns, with particular emphasis on the occurrence of instability conditions and the dependable compressive strain of the column prior to actual buckling of the reinforcing bars. In this model, the dilation of the concrete core and concrete cover are described through the following equation (Eq. (4))[2]

$$\varepsilon_r\left(\varepsilon_{con}, f_l\right) = \frac{E_{con}\varepsilon_{con} - f_c\left(\varepsilon_{con}, f_l\right)}{2\beta f_c\left(\varepsilon_{con}, f_l\right)}, \quad \beta = \frac{5700}{\sqrt{|f_{co}|}} - 500 \tag{4}$$

Thus, the lateral pressure of the FRP jacket confining the concrete cover has been taken into account and, by relating the critical buckling conditions with the onset of significant strength loss of the concrete cover, the effect of the confining pressure exerted by the jacket in delaying the occurrence of buckling of the longitudinal bars can be evaluated. Therefore, the critical buckling conditions are delayed, depending on how circumferentially stiff the jacket is, which accordingly delays the failure of the concrete cover that laterally supports the longitudinal bar. This onset of loss of resistance in concrete has been proven to be the point when the net volumetric strain $\varepsilon_v$ of the material becomes equal to zero.[10] In circular sections, this occurs when

$$\varepsilon_V = 0 \Rightarrow 2 \cdot \varepsilon_r = \varepsilon_{con} \Rightarrow \nu = 0.5 \tag{5}$$

However, another condition that should be valid for the attainment of critical instability conditions of the longitudinal bars in the high confining stress states under consideration is the occurrence of compression yielding of the longitudinal bar. Regarding this step, it is interesting to note, with reference to Fig. 3 for a given concrete strength, the point where the volumetric ratio becomes zero moves forward into higher axial compression strain values with increasing confining pressures. Thus, the difference in the lateral behavior of the concrete cover (confined with the jacket's pressure) and the concrete core (confined by both the steel's and FRP's pressure) should also be considered.

As shown in previous studies,[7,11] the buckling length $L_{buck}$ and the $L_{buck}/D_b$ ratio are critical parameters for the post-buckling behavior of longitudinal bars under compression. In cases of columns constructed with obsolete codes with the spacing of the stirrups ranging between 7.87 and 19.68 in. (200 and 500 mm) (buckling length) and bar diameters from 0.47 to 0.79 in. (12 to 20 mm), the $L_{buck}/D_b$ ratio ranges from 10 to 42. Apart from old-type columns, however, the assumption that the buckling length is equal to the spacing of the stirrups in an RC column does not hold true in all cases[12] and it may extend over more than single-tie spacing. To take this behavior into account (cases of reinforcement repair and FRP retrofit), the following procedure is suggested.

The longitudinal bar is modeled as a pin-ended bar supported along its length by an elastic foundation, as shown in Fig. 4. The foundation modulus is $k$ (N/mm$^2$) and it is such that when the bar deflects by an amount $u$, a restoring force is exerted by the foundation normal to the bar. The governing homogeneous differential equation and the associated eigenvalue problem are

$$EIu^{iv} + Pu'' + ku = 0 \tag{6}$$

$$P_{cr} = \frac{\pi^2 EI_{red}}{L_{buck}^{\ 2}}\left[m^2 + \frac{1}{m^2}\left(\frac{kL_{buck}^{\ 4}}{\pi^4 EI_{red}}\right)\right] \tag{7}$$

Note that if $k = 0$ (which occurs upon yielding of the stirrups), the minimum value of $P_{cr}$ becomes the classical Euler buckling load. To determine the critical load, the buckling mode $m$ equal to 1 should be used. The stiffness $k$ representing the supporting system of stirrups could be calculated as follows

$$k = n \cdot \frac{E_s \cdot A_{sh}}{L_{buck} \cdot \pi \cdot D_{core}},\ L_{buck} = (n+1)S \tag{8}$$

$$EI_{red} = 0.5 \cdot E_s \cdot I_b \cdot \sqrt{\frac{f_{yl}}{400}} \tag{9}[12]$$

The solution of the previous problem is obtained by setting the critical load of the bar equal to its yield force; in this case, the only unknown is the number $n$ of the stirrups $n$ over the buckling length. Therefore, by solving Eq. (7) for $n$, the buckling length is determined. The value of $n$ may be rounded to the nearest integer because the pin-ended bar segment engaged in buckling is assumed to span between successive inflection points of the real deformed shape. If convergence is not possible for $n > 1$, the buckling length is taken as equal to the spacing of the stirrups.

In conclusion, after the critical conditions of a longitudinal compressive bar have been attained (this is assumed to coincide upon compression yielding of the bar and the Poisson's coefficient at the concrete cover exceeding the value of 0.5), the buckling length of the bar is determined. Then, based on the model by Bae et al.,[7] who have related the axial strain with the transversal displacement of the buckled longitudinal bar for a given $L_{buck}/D_b$ ratio, the transversal displacement of the bar $u$ is calculated (Table 1). Because, for a longitudinal bar embedded in an RC member, axial shortening of the bar means the same amount of shortening for the surrounding concrete mass,[13] the axial strain in the bar is taken as equal with the axial strain of concrete. Finally, the jacket's circumferential strain due to buckling is determined as follows

$$\varepsilon_{c.buck} = \frac{2 \cdot \pi \cdot |u - c|}{\pi \cdot D} \le \varepsilon_{j.rup.coup},\ \text{(full wrapping)} \tag{10}$$

$$\varepsilon_{c.buck} = \frac{2 \cdot \pi \cdot \left|u - \frac{c}{2}\right|}{\pi \cdot D} \le \varepsilon_{j.rup.coup},\ \text{(partial wrapping)} \tag{11}$$

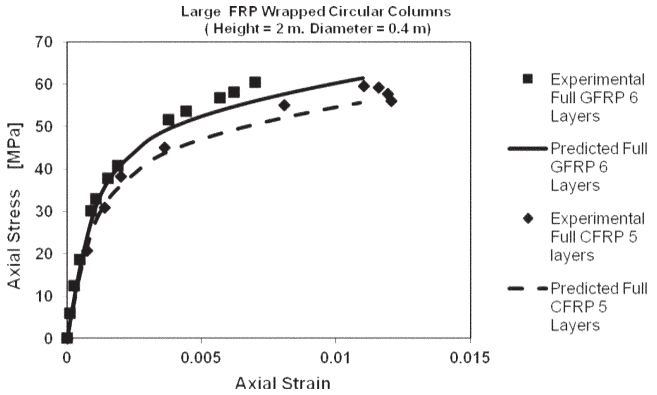


*Fig. 5—Correlation with experimental results.[6] (Note: 1 MPa = 145 psi; 1 m = 3.28 ft.)*

It follows from the previous equations (Eq. (10) and (11)) that a tolerance equal to the concrete cover for full wrapping and half of the concrete cover for partial wrapping is given before the initiation of the jacket's strains due to buckling of the longitudinal bars because the concrete cover should be severely cracked in the case of full wrapping, and some spalling could appear in the case of partial wrapping. Because the displacement of the buckled longitudinal bar could be high and the phenomenon locally affects the jacket where the FRP material behavior could be considered linear-elastic, the results are compared to the deformation capacity of tensile coupons (dilation strains and buckling strains are studied independently).

In the proposed algorithm detailed previously, the failure criterion is used in two steps. First, the circumferential strain due to dilation of concrete under compression is compared to a reduced FRP tensile coupon strain; second, the induced circumferential strains due to buckling, which locally accelerate the jacket's rupture, are compared to the deformation capacity of flat FRP tensile coupons. If one of these conditions is fulfilled, the iteration procedure is terminated.

## COMPARISON OF PREDICTIONS AND EXPERIMENTAL RESULTS

Three experimental studies are included in this work for validation of the proposed iterative procedure. The first[6] is one of the few extensive experimental studies on large-scale FRP-wrapped circular columns where different FRP configurations have been applied for identical embedded steel reinforcement. It includes eight large-scale columns subjected to axial loading. The columns had a total length of 6.56 ft (2 m), a longitudinal reinforcement ratio of 0.9%, and 0.32 in. (8 mm) diameter stirrups spaced at 5.51 in. (140 mm). All columns had a circular cross section 15.75 in. (400 mm) in diameter. Different types of FRP reinforcement (carbon fiber-reinforced polymer [CFRP], glass fiber-reinforced polymer [GFRP], and hybrid fiber-reinforced polymer [HFRP]) were used to confine the columns. The comparison seems to be satisfactory (Fig. 5 and 6), although the solution has moderate success in resolving the problem of predicting the actual instance of the jacket's failure in terms of axial and circumferential ultimate strains. Some clarifications are in order for the last graph (Fig. 7), which illustrates the model's estimations of the circumferential strains in the FRP jacket owing to concrete dilation and buckling of longitudinal bars at the ultimate axial strain reported in the tests for each specimen. These values are accordingly compared to the experimental rupture strain of the jacket (from strain

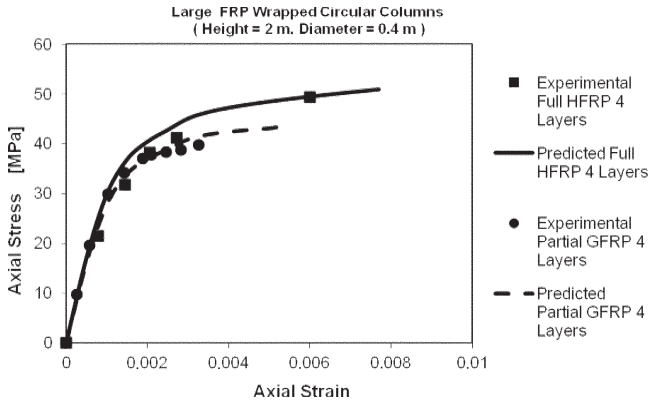


*Fig. 6—Correlation with experimental results.[6] (Note: 1 MPa = 145 psi; 1 m = 3.28 ft.)*

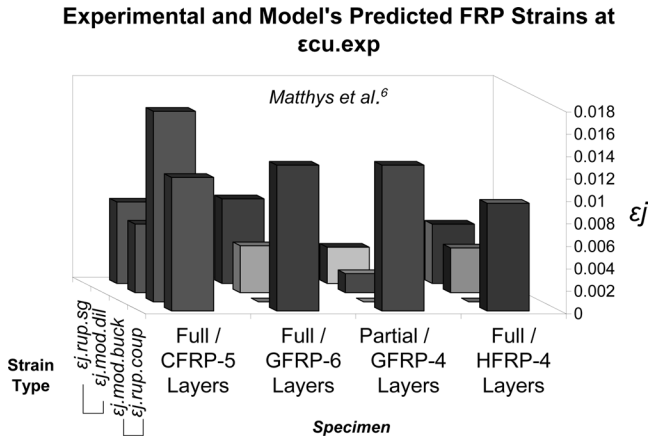


*Fig. 7—Correlation with experimental results.[6]*

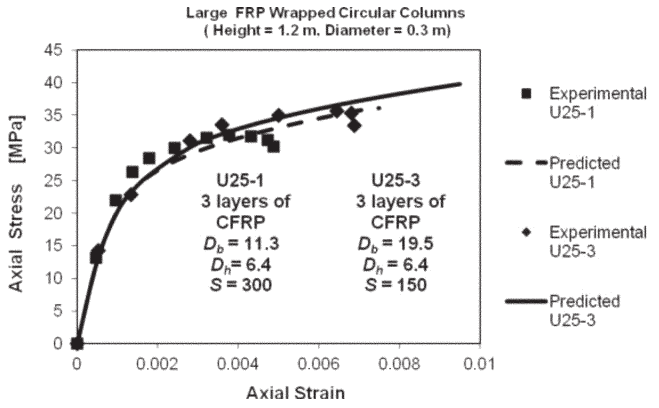


*Fig. 8—Correlation with experimental results.[14] (Note: 1 MPa = 145 psi; 1 m = 3.28 ft.)*

gauges) and the deformation capacity of the flat tensile coupons that was reported.

The second experimental study[14] includes 16 RC columns having a circular section 11.81 in. (300 mm) in diameter and 3.936 ft (1200 mm) high. These columns were confined by means of carbon-epoxy sheets and loaded concentrically in axial compression. The effects of various parameters on the structural behavior of the confined concrete columns are investigated. These parameters included the concrete strength, longitudinal steel reinforcement, steel stirrups, steel corrosion, and concrete damage while the FRP configuration was kept constant. The comparison between the model estimates

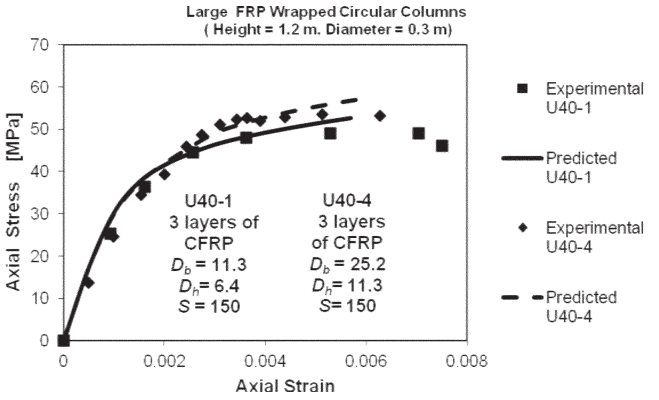


*Fig. 9—Correlation with experimental results.[14] (Note: 1 MPa = 145 psi; 1 m = 3.28 ft.)*

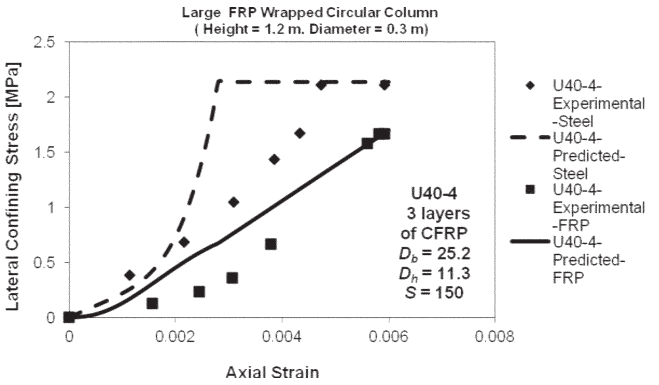


*Fig. 10—Correlation with experimental results.[14] (Note: 1 MPa = 145 psi; 1 m = 3.28 ft.)*

and experimental results depicted in Fig. 8 and 9 in this case could also be characterized as satisfactory—more so due to the fact that, in this experimental study, the lateral pressures from both confining materials (steel and FRP) are provided based on circumferential strains obtained by strain gauges applied on both the FRP jacket and steel ties. (It should be noted that the horizontal strain gauges on the jacket were located midway between two successive stirrups.) Among the 16 specimens, in only one case (Specimen U40-4), the pressures coming from the ties were evidently higher than those of the FRP jacket, which the model was able to detect (Fig. 10).

The third and last experimental study[15] contains a series of cyclic loading tests that were conducted on six RC column specimens 15.75 in. (400 mm) in diameter and 4.43 ft (1.350 mm) in effective height. The specimens were grouped into the A-series and B-series. Each series consisted of three specimens each; one was as-built, while the second and the third were wrapped laterally by CFRP with a single layer and two layers, respectively. The tie reinforcement ratio was 0.256% (5.91 in. [150 mm] spacing) for the A-series and 0.128% (11.81 in. [300 mm] spacing) for the B-series. Figures 11 through 14 depict the comparison with the two groups of cyclic tests on bridge piers having different levels of confinement in terms of lateral steel reinforcement and FRP jacketing. The modeling of the bridge piers was the same as in the original paper and was performed using the "MatLab Finite Elements for Design Evaluation and Analysis of Structures" (FEDEAS Lab)[16] developed by F. C. Filippou. While in the original proposal the fiber section had to be divided in the concrete core and concrete cover

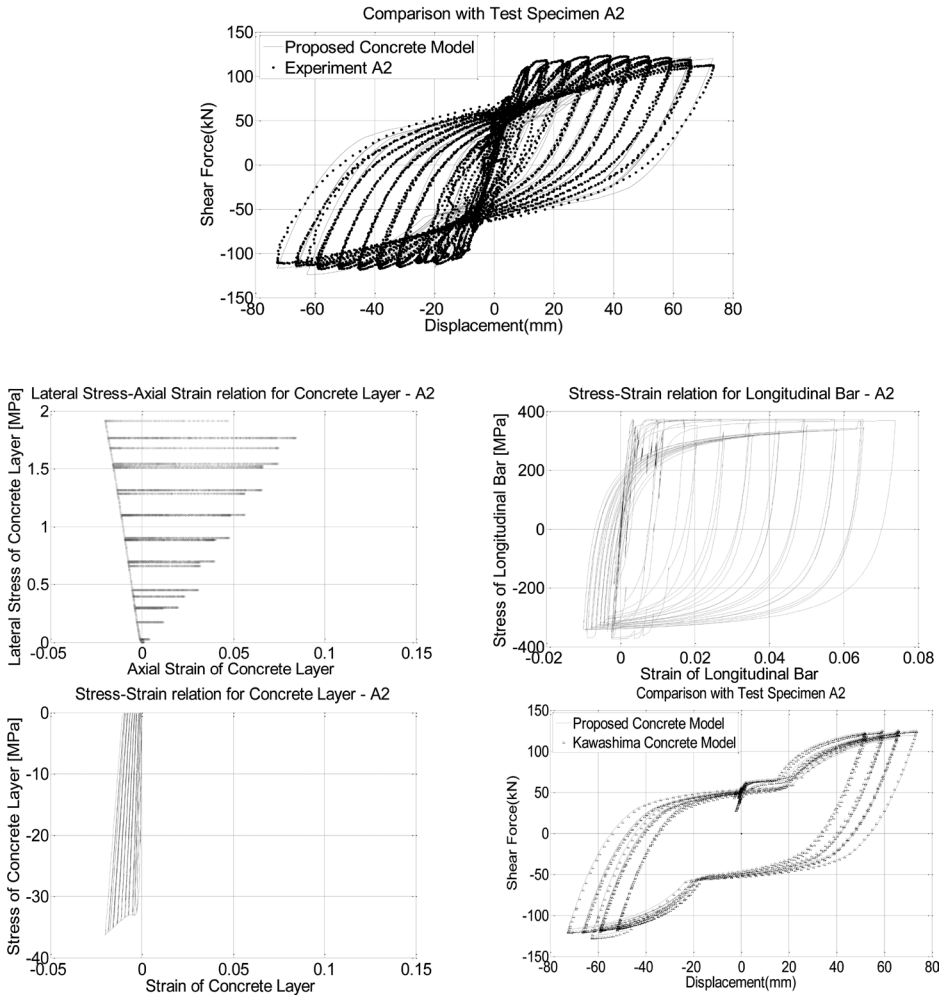


*Fig. 11—Correlation with experimental results A2.[15] (Note: 1 MPa = 145 psi; 1 mm = 0.0394 in.; 1 kN = 0.2248 kips.)*

and two different stress-strain relations were applied for the concrete core (confined by both FRP and steel) and concrete cover (confined by only the FRP), in this work, because the material response is already averaged based on the different responses of those two regions, the same stress-strain law is applied for each fiber. This fact gives a clear advantage to the proposed model. In addition to the force-displacement response of the cantilever columns, the response in the level of the section for each specimen in terms of material stress-strain hysteresis is provided. It can be seen that the agreement is very close to the experimental one, with some deviation concentrated on the parts of reloading after reversal of the imposed displacement. This difference in response in terms of modeling can be explained based on the way the cracks on the concrete surface are described in the level of the material model. Because the crack is described as a two-event phenomenon (open or closed) (in reality, this is not the case due to imperfect crack closure), the contribution of concrete while the longitudinal steel reinforcement is in compression and the crack is closing gives this deviation in the response. The comparison with the originally proposed model of this experimental study is, impressively, the same. However, the proposed model rationally describes the procedure of the passive confinement based on the calculation of the lateral concrete expansion in terms of the different levels of lateral pressures coming from the two different materials (steel and FRP). Moreover, the active (constant lateral pressure) confinement model proposed by Gallardo-Zafra and Kawashima[15] is based on regression analysis of the experimental results of cylindrical specimens under compression, and it is specifically calibrated for CFRP. Finally, the model does not consider the confinement effect of the longitudinal reinforcement and the effect of partial confinement due to the vertical arching action of the adjacent stirrups along the member or cases of partial FRP wrapping of the column.

Some studies[15,17] have reported a different behavior (softening) in respect to the already-recognized bilinear one[4] for FRP- and steel-confined concrete in circular RC sections. The authors attribute this to the small scale of the RC specimens used, but the most important explanation that could lead to those results is the influence of concrete strength. According to Mandal et al.,[18] the FRP wraps provide a substantial increase in strength and ductility for low-to-medium-strength concrete, which shows a bilinear stress-strain response with strain hardening. For high-strength concrete, however, enhancement in strength is very limited, with hardly any improvement in ductility. The response in this case shows a steep post-peak strain softening.

## CONCLUSIONS

Based on the results of this analytical investigation and the comparison of the predictions with the experimental studies under consideration, the following conclusions are drawn:

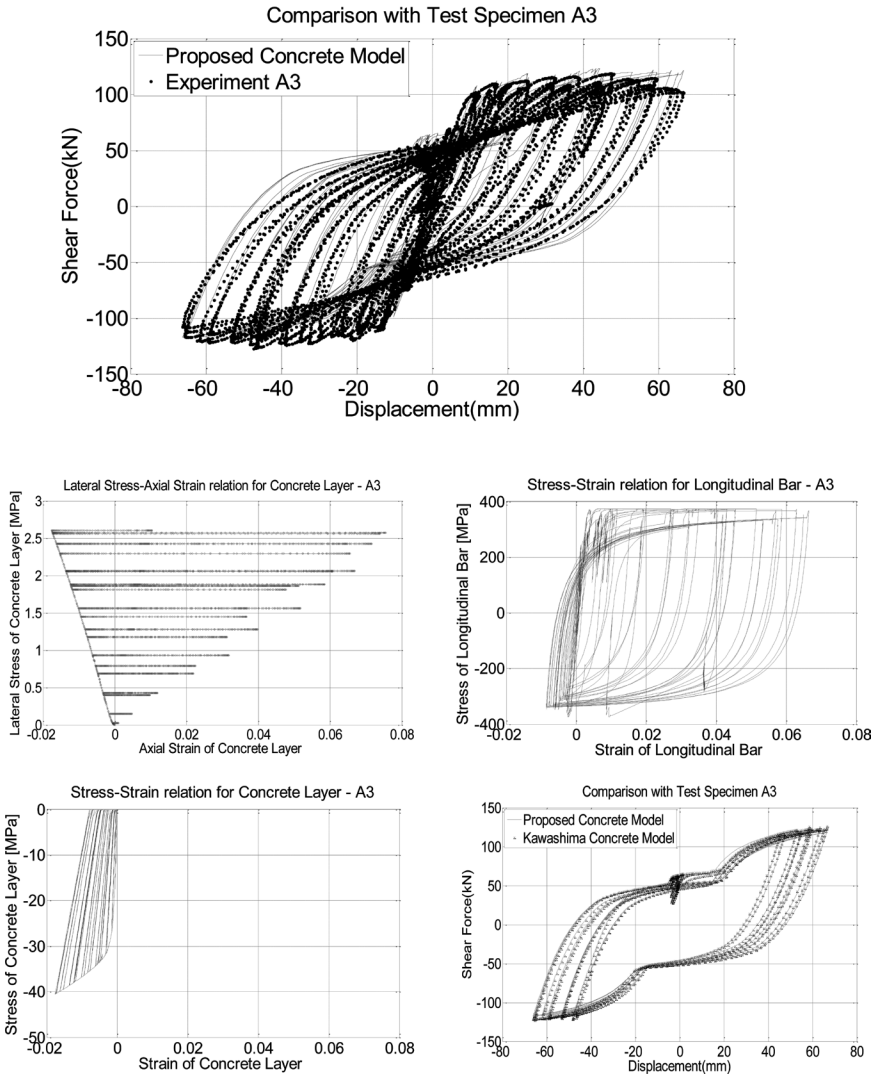


*Fig. 12—Correlation with experimental results A3.[15] (Note: 1 MPa = 145 psi; 1 mm = 0.0394 in.; 1 kN = 0.2248 kips.)*

1. The *fib* FRP-confined concrete model[1,2] was enhanced to take into account the confining effect of the already-existing steel reinforcement when retrofitting an RC column with FRP jacketing. To this end, the transverse steel reinforcement was considered, not as imposing a constant value of confining pressure but, rather, following the steel stress-strain law at each deformation step in accordance with the BGL model[3] while also considering the confining contribution of longitudinal reinforcement.

2. In addition, compatibility in the lateral direction—inward for confining pressures and outward for lateral strains—between the two confining materials (FRP and steel) was established. Through this approach, the difference in the lateral behavior of the concrete cover (confined with the jacket's pressure) and the concrete core (confined by both the steel's and FRP's pressure) was considered.

3. This also allows the application of the model in cases of reinforcement repair and FRP retrofit, where two different concrete strengths should be considered: one for the new layer of concrete applied externally and the other for the old concrete in the concrete core, which may also be cracked due to former seismic loading.

4. Finally, a two-condition failure criterion was incorporated regarding the dilation of concrete and buckling of longitudinal bars as independent events. Correlation with experimental results seems to be satisfactory, although the model has moderate success in predicting the actual instance of rupture of the FRP jacket.

## ACKNOWLEDGMENTS

This work was carried out with the financial support of the RELUIS Program (Department of Civil Protection).

## NOTATION

$A_{core}$ = total area of concrete core of circular section
$A_{cover}$ = total area of concrete cover of circular section
$A_b$ = total area of longitudinal steel reinforcement
$A_g$ = gross area of section
$A_{sh}$ = area of steel stirrup
$A_{tot}$ = total area of circular section
$C$ = circumference of circular section
$c$ = concrete cover
$D$ = section's diameter
$D_b$ = longitudinal steel bar diameter
$D_{core}$ = diameter of concrete core
$D_h$ = hoop's diameter
$E_{con}$ = modulus of elasticity for concrete
$E_{con.core}$ = modulus of elasticity for concrete core
$E_j$ = jacket's modulus
$E_s$ = modulus of elasticity for steel
$E_{sec}$ = secant modulus of concrete

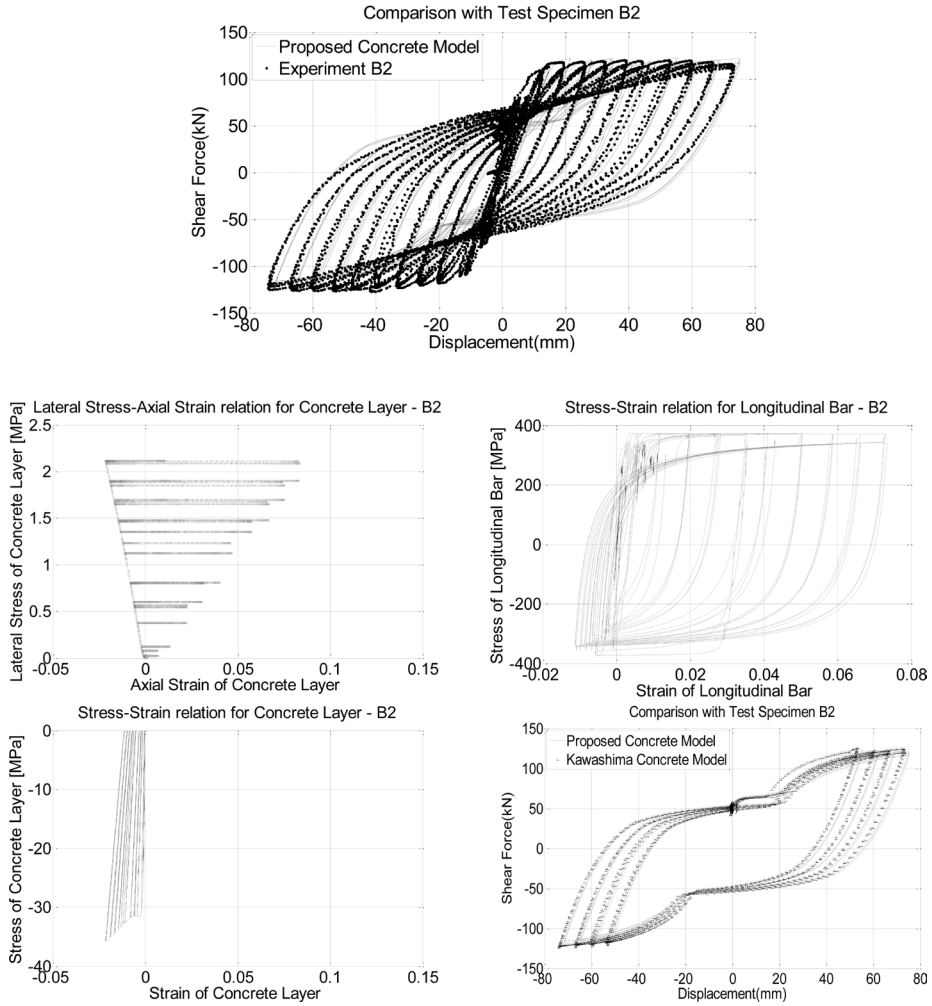


*Fig. 13—Correlation with experimental results B2.[15] (Note: 1 MPa = 145 psi; 1 mm = 0.0394 in.; 1 kN = 0.2248 kips.)*

$EI$ = flexural rigidity of foundation
$EI_{red}$ = reduced flexural rigidity of steel longitudinal bar
$f_c$ = axial concrete stress
$f_{c.av}$ = average axial concrete stress
$f_{c.core}$ = axial concrete core stress
$f_{c.cover}$ = axial concrete cover stress
$f_{cc}$ = confined concrete strength
$f_{cc.core}$ = axial confined concrete core stress
$f_{cc.cover}$ = axial confined concrete cover stress
$f_{co}$ = concrete strength
$f_l$ = lateral confining pressure
$f_{l.core}$ = lateral confining pressure of concrete core
$f_{l.cover}$ = lateral confining pressure of concrete cover
$f_{l.steel}$ = lateral confining pressure of steel reinforcement
$f_{yh}$ = yielding stress of stirrup
$f_{yl}$ = yielding strength of longitudinal bar
$I_b$ = longitudinal bar's moment of inertia
$k$ = foundation stiffness
$k_j$ = partial wrapping coefficient
$k_{sl}$ = partial confinement coefficient for steel
$L_{buck}$ = buckling length
$m$ = buckling mode
$n$ = number of stirrups
$P$ = axial load along length of foundation
$P_{cr}$ = critical load
$R$ = radius of circular section
$R_{core}$ = radius of concrete core
$r$ = parameter that compares tangent modulus of elasticity of concrete to secant modulus of elasticity
$S$ = spacing of steel stirrups
$S_j$ = jacket's clear spacing
$t_j$ = thickness of jacket
$u$ = lateral displacement of longitudinal steel bar
$v$ = Poisson's coefficient for concrete
$v_o$ = initial Poisson's coefficient for concrete
$w$ = reduction factor
$x$ = parameter that compares concrete's axial strain to strain at confined concrete's strength
$\beta$ = property of concrete evaluated as function of unconfined concrete strength
$\Delta C$ = change in circumference of circular section
$\varepsilon_c$ = circumferential strain
$\varepsilon_{c.buck}$ = circumferential strain due to buckling of longitudinal bar
$\varepsilon_{c.core}$ = circumferential strain of core
$\varepsilon_{cc}$ = concrete's axial strain at confined concrete's strength
$\varepsilon_{co}$ = concrete's axial strain at unconfined concrete's strength
$\varepsilon_{con}$ = concrete's axial strain
$\varepsilon_{cu.exp}$ = ultimate axial strain measured experimentally
$\varepsilon_j$ = FRP jacket's strain
$\varepsilon_{j.mod.buck}$ = jacket's strain due to buckling of longitudinal bar calculated by model
$\varepsilon_{j.mod.dil}$ = jacket's strain due to concrete's dilation calculated by model
$\varepsilon_{j.rup.coup}$ = rupture strain of tensile FRP coupon
$\varepsilon_{j.rup.sg}$ = jacket's rupture strain measured from strain gauges
$\varepsilon_{sh}$ = strain of steel stirrup
$\varepsilon_{shu}$ = ultimate steel hoop's strain
$\varepsilon_{sl}$ = axial strain in bar
$\varepsilon_r$ = radial strain
$\varepsilon_{r.core}$ = radial strain of core
$\varepsilon_{r.cover}$ = radial strain of cover
$\varepsilon_v$ = volumetric concrete strain
$\varepsilon_{yh}$ = yielding strain of stirrup
$\theta$ = slope of line that relates transverse displacement and axial strain of buckling bar

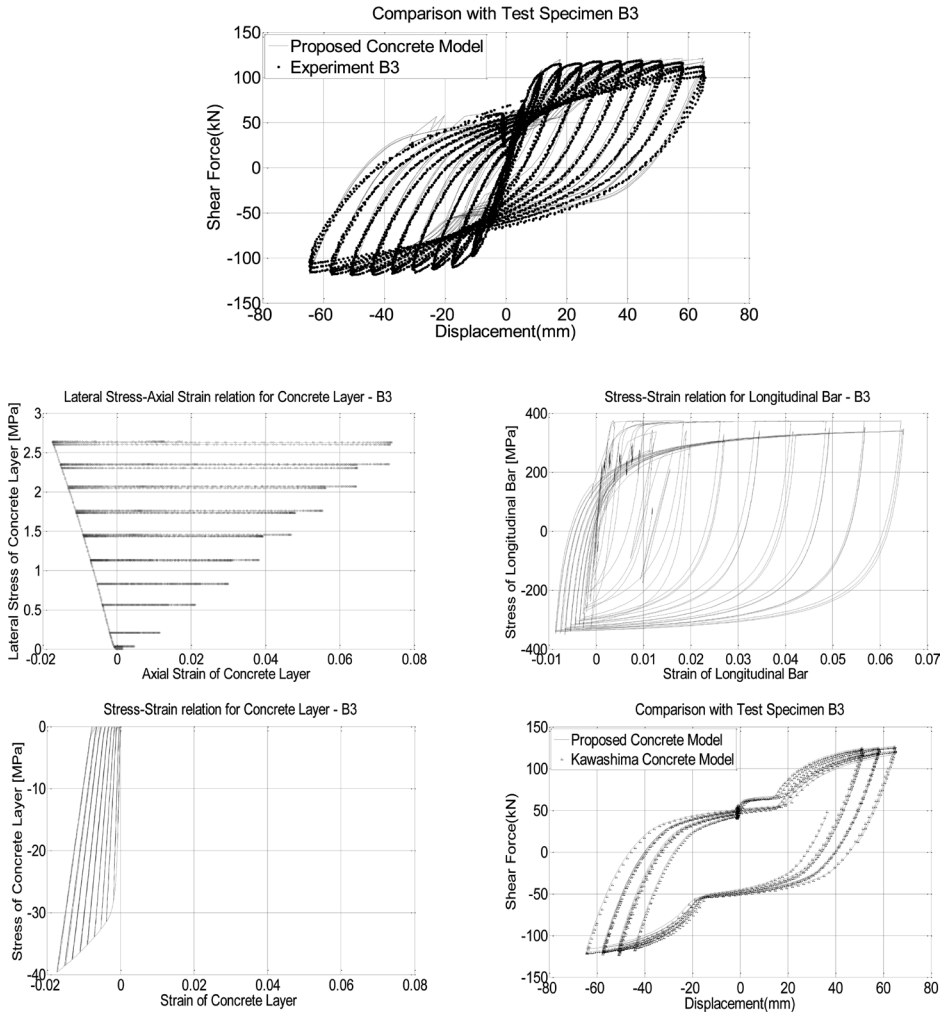


*Fig. 14—Correlation with experimental results B3.[15] (Note: 1 MPa = 145 psi; 1 mm = 0.0394 in.; 1 kN = 0.2248 kips.)*

$\rho_j$ = FRP jacket's volumetric ratio
$\rho_{sh}$ = steel hoop's volumetric ratio
$\xi_l$ = coefficient taking into account confining effect of longitudinal bar
$\xi_{st}$ = coefficient taking into account confining effect of stirrup

## REFERENCES


1. Federation Internationale du Beton (*fib*), "Externally Bonded FRP Reinforcement for RC Structures," *14th* fib *Bulletin,* Lausanne, Switzerland, 2001, pp. 1-139.

2. Spoelstra, M. R., and Monti, G., "FRP-Confined Concrete Model," *Journal of Composites for Construction*, V. 3, No. 3, Aug. 1999, pp. 143-150.

3. Braga, F.; Gigliotti, R.; and Laterza, M., "Analytical Stress-Strain Relationship for Concrete Confined by Steel Stirrups and/or FRP Jackets," *Journal of Structural Engineering*, ASCE, V. 132, No. 9, Sept. 2006, pp. 1-15.

4. Carey, S. A., and Harries, K. A., "Axial Behavior and Modeling of Confined Small-, Medium-, and Large-Scale Circular Sections with Carbon Fiber-Reinforced Polymer Jackets," *ACI Structural Journal*, V. 102, No. 4, July-Aug. 2005, pp. 596-604.

5. Lam, L., and Teng, J. G., "Ultimate Condition of Fiber Reinforced Polymer-Confined Concrete," *Journal of Composites for Construction*, V. 8, No. 6, Nov.-Dec. 2004, pp. 539-548.

6. Matthys, S.; Toutanji, H.; Audenaert, K.; and Taerwe, T., "Axial Load Behavior of Large-Scale Columns Confined with Fiber-Reinforced Polymer Composites," *ACI Structural Journal*, V. 102, No. 2, Mar.-Apr. 2005, pp. 258-267.

7. Bae, C.; Mieses, A. M.; and Bayrak, O., "Inelastic Buckling of Reinforcing Bars," *Journal of Structural Engineering*, ASCE, V. 131, No. 2, Feb. 2005, pp. 314-321.

8. Sheikh, S. A., and Yao, G., "Seismic Behavior of Concrete Columns Confined with Steel and Fiber-Reinforced Polymers," *ACI Structural Journal*, V. 99, No. 1, Jan.-Feb. 2002, pp. 72-80.

9. Tastani, S. P.; Pantazopoulou, S. J.; Zdoumba, D.; Plakantaras, V.; and Akritidis, E., "Limitations of FRP Jacketing in Confining Old-Type Reinforced Concrete Members in Axial Compression," *Journal of Composites for Construction*, V. 10, No. 1, Jan.-Feb. 2006, pp. 13-25.

10. Pantazopoulou, S. J., and Mills, R. H., "Microstructural Aspects of the Mechanical Response of Plain Concrete," *ACI Materials Journal*, V. 92, No. 6, Nov.-Dec. 1995, pp. 605-616.

11. Monti, G., and Nuti, C., "Nonlinear Cyclic Behavior of Reinforcing Bars Including Buckling," *Journal of Structural Engineering*, ASCE, V. 118, No. 12, Dec. 1992, pp. 3268-3284.

12. Dhakal, P. R., and Maekawa, K., "Reinforcement Stability and Fracture of Cover Concrete in Reinforced Concrete Members," *Journal of Structural Engineering*, ASCE, V. 128, No. 10, Oct. 2002, pp. 1253-1262.

13. Pantazopoulou, S. J., "Detailing for Reinforcement Stability in RC Members," *Journal of Structural Engineering*, ASCE, V. 124, No. 6, June 1998, pp. 623-632.

14. Demers, M., and Neale, K. W., "Confinement of Reinforced Concrete Columns with Fibre-Reinforced Composite Sheets—An Experimental Study," *Canadian Journal of Civil Engineering*, V. 26, 1999, pp. 226-241.

15. Gallardo-Zafra, R., and Kawashima, K., "Analysis of CFRP RC Bridge Columns under Lateral Cyclic Loading," *Journal of Earthquake Engineering*, V. 13, 2009, pp. 129-154.

16. Filippou, F. C., "FEDEAS Nonlinear Static and Dynamic Analysis from Research to Practice," *Proceedings of the Conference on Analysis and Computation*, Chicago, IL, 1996, pp. 31-42.

17. Khaloo, A.; Javid, Y.; and Tazarv, M., "Experimental Study of the Internal and External (FRP) Confinement Effect on Performance of Compressive Concrete Members," *14th World Conference on Earthquake Engineering (14th WCEE),* Beijing, China, Oct. 12-17, 2008, pp. 1-8.

18. Mandal, S.; Hoskin, A.; and Fam, A., "Influence of Concrete Strength on Confinement Effectiveness of Fiber-Reinforced Polymer Circular Jackets," *ACI Structural Journal*, V. 102, No. 3, May-June 2005, pp. 383-392.